Indicator of Small Calcification Detection in Ultrasonography using Decorrelation of Forward Scattered Waves

Hirofumi Taki, Takuya Sakamoto, Makoto Yamakawa, Tsuyoshi Shiina, and Toru Sato

Abstract—For the improvement of the ability in detecting small calcifications using Ultrasonography (US) we propose a novel indicator of calcifications in an ultrasound B-mode image without decrease in frame rate. Since the waveform of an ultrasound pulse changes at a calcification position, the decorrelation of adjacent scan lines occurs behind a calcification. Therefore, we employ the decorrelation of adjacent scan lines as an indicator of a calcification. The proposed indicator depicted wires 0.05 mm in diameter at 2 cm depth with a sensitivity of 86.7% and a specificity of 100%, which were hardly detected in ultrasound B-mode images. This study shows the potential of the proposed indicator to approximate the detectable calcification size using an US device to that of an X-ray imager, implying the possibility that an US device will become a convenient, safe, and principal clinical tool for the screening of breast cancer.

Keywords—Ultrasonography, Calcification, Decorrelation, Forward scattered wave

I. INTRODUCTION

ULTRASONOGRAPHY (US) is a convenient and safe imaging tool with an excellent ability in depicting soft tissues; however, the ability of US in detecting a calcification is insufficient compared with X-ray computed tomography (CT) and other X-ray imaging techniques. For the evaluation of genitourinary calcifications, X-ray computed tomography (CT) has become the primary imaging modality, causing US to play a secondary role [1]. In general, US has difficulty detecting small calcifications 3.0 mm or less in size [2]. US is also used as an adjunct to mammography in the diagnosis of breast cancer [3]–[6].

The purpose of this study is to propose a useful indicator to detect small calcifications using US devices. The waveform of the echo behind a small calcification, being accompanied no acoustic shadowing, is supposed to be changed by the forward scattered wave originating at the calcification. In a recent study,

H. Taki, T. Sakamoto, and T. Sato are with the Graduate School of Informatics, Department of Communications and Computer Engineering, Kyoto University, Kyoto, Japan (e-mail: hirofumi.taki@mb6.seikyou.ne.jp).
M. Yamakawa is with the Advanced Biomedical Engineering Research Unit, Kyoto University, Kyoto, Japan.
T. Shiina is with the Graduate School of Medicine, Kyoto University, Kyoto, Japan.

we reported that the waveform change of the echo caused by a calcification results in the decorrelation between the echoes received at adjacent scan lines [7], [8]. These reports indicate that the existence of a small calcification is predictable from the waveform difference between adjacent scan lines by calculating cross-correlation coefficients. In this paper, we propose a novel indicator of calcifications and evaluate the method experimentally using a commercial US device.

II. MATERIALS AND METHODS

To detect calcifications, we utilize the decrease of cross-correlation coefficients between adjacent scan lines. Since the decrease of cross-correlation coefficients correspond to the phase change of the echo caused by a calcification, the proposed method is supposed to have higher sensitivity for the depiction of a calcification than acoustic shadowing, corresponding to the intensity change caused by a calcification. When a calcification exists in scan line, the waveform of an ultrasound pulse changes considerably at the calcification position in both transmit and receive paths, as shown in Fig. 1. Therefore the echo waveform of a scan line with a calcification is significantly different from that without a calcification, where the echoes return from the calcification or a range behind it. This indicates that a decrease in cross-correlation coefficients can predict the existence of a calcification.

When a small calcification exists close to a layered structure, e.g. a calcification in a mammary duct and that on a gallbladder wall, the high-intensity specular echo from the layered structure severely interferes with the depiction of the calcification in a B-mode image. In this paper we thus investigate the performance of the proposed method when a layered structure exists just behind a calcification, one of the most difficult cases to detect a small calcification in a B-mode image. This section explains the detailed process of the proposed method.

A. Real Data Oversampling

Medical acoustic imagers utilize quadrature detectors to acquire IQ data. The detection is equivalent to the multiplication processes between a received signal and two sinusoidal waves, where the phase difference of the two sinusoidal waves is 90 degrees and their center frequency is equal to transmit center frequency. However the IQ data

World Academy of Science, Engineering and Technology
International Journal of Biomedical and Biological Engineering
Vol:4, No:11, 2010

correspond with the real and imaginary components of the received signal only at the transmit center frequency. When a broad-band signal is employed the so-called IQ data are really the oversampled real data with the sampling frequency of four times the transmit center frequency [9]. For the broad-band signal processing we convert the IQ data to the oversampled real data.

$$g(x, z - \frac{\Delta Z}{2}) = (-1)^m g_1(x, z), \qquad (1)$$

$$g(x, z) = (-1)^m g_Q(x, z), \qquad (2)$$

$$z = m\Delta Z, \qquad (3)$$

where x and z are the lateral and vertical components, respectively, of a measurement point on a B-mode image, $g(x, z)$ is the oversampled real datum at $P(x, z)$, a pixel in a B-mode image, ΔZ is the range interval, $g_1(x, z)$ and $g_Q(x, z)$ are respectively the IQ data at $P(x, z)$, and m is an integer. When the correlation of adjacent scan lines becomes the maximum value in the case that the correlation windows of the two scan lines are located at the same position, the cross-correlation between adjacent scan lines of oversampled real data is

$$r(x + \frac{\Delta X}{2}, z) \qquad (4)$$
$$= \sum_z \{g(x, z - \frac{\Delta Z}{2}) g(x + \Delta X, z - \frac{\Delta Z}{2}) + g(x, z)g(x + \Delta X, z)\},$$

where ΔX is the scan line interval. In this case the cross-correlation between adjacent scan lines of IQ data is expressed by
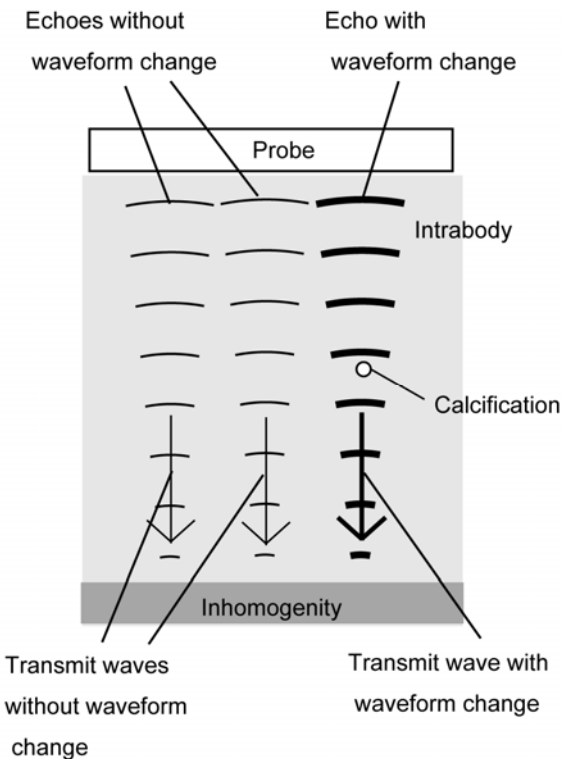

Fig. 1 Waveform change of an ultrasound pulse originating from a calcification, causing the decrease of correlation between adjacent scan lines.

$$r_c(x + \frac{\Delta X}{2}, z) = \left| \sum_z r(x + \frac{\Delta X}{2}, z) \right. \qquad (5)$$
$$+ j\sum_z \{-g(x, z - \frac{\Delta Z}{2})g(x + \Delta X, z) + g(x, z)g(x + \Delta X, z - \frac{\Delta Z}{2})\} \left. \right|.$$

The error of the cross-correlation caused by the utilization of IQ data increases when the correlation is calculated by a pair of scan lines with low correlation. This indicates the validity of the utilization of the real data oversampling for the calculation of cross-correlation.

B. Cross-correlation between Adjacent Scan Lines

The proposed indicator of a calcification utilizes the decorrelation of adjacent scan lines; however, a correlation coefficient is suppressed by not only a calcification, but also noise. When signals cut out by correlation windows have low signal-to-noise ratio (SNR), the effect of noise on the correlation coefficients is emphasized, interfering with the detection of the decrease on correlation coefficients caused by a calcification. In this study, we employ an echo intensity threshold and a modified Wiener filter to decrease the influence of noise on cross-correlation coefficients. An echo intensity threshold eliminates the signal with low SNR, and a cross-correlation coefficient with a modified Wiener filter suppresses the influence of noise on the cross-correlation coefficient. The proposed method calculates a cross-correlation r_W when both the adjacent signals cut out by correlation windows are over an intensity threshold I_t.

$$l_t = \alpha n I_0, \qquad (6)$$

$$r_W(x + \frac{\Delta X}{2}, z)$$
$$= \max_l \frac{\sum_{z'=z_1}^{z_2} g(x, z') g(x + \Delta X, z' + l\Delta Z_S) + \beta n I_0}{\sqrt{\sum_{z'=z_1}^{z_2} |g(x, z')|^2 \sum_{z'=z_1}^{z_2} |g(x + \Delta X, z' + l\Delta Z_S)|^2} + \beta n I_0}, \qquad (7)$$

where α and β are positive numbers, n is the size of correlation window width, I_0 is the average pixel intensity in a region of interest (ROI), ΔZ_S is the scan interval of a correlation window, z_1 and z_2 are the minimum and maximum of the z coordinates of a correlation window behind $P(x, z)$. In this study the correlation window width was 5 mm and $z_1 = z$. We examined the performance of the proposed indicator employing the nine combinations of parameters α and β, where $\alpha = 0$, -3, and -6 dB and $\beta = 0$, -10, and -20 dB.

C. Indicator of Calcifications Using Decorrelation between Scan Lines

A region with significantly lower cross-correlation compared with common tissues indicates that a calcification exists in front of the region. To examine cross-correlation coefficients of common tissues except calcifications, we calculate the average μ and the standard deviation σ of the top 90% of the correlation coefficients in a ROI. The proposed indicator depicts the regions with lower correlation coefficients than $\mu - \gamma\sigma$, where γ is a positive number. In this study we examined the cases of $\gamma = 10$, 7.5, and 5, where a larger value of

World Academy of Science, Engineering and Technology
International Journal of Biomedical and Biological Engineering
Vol:4, No:11, 2010

γ means a severer correlation threshold.

The proposed indicator calculates a correlation profile from a single B-mode image. This indicates that the proposed method involves no decrease in frame rate when a sufficient signal processing unit is employed.

D. Experimental Setup

Experiments were conducted using a Hitachi EUB-8500 (Hitachi, Tokyo, Japan) US device with a 7.5 MHz linear array probe whose scan line interval is approximately 0.13 mm. We prepared nine calcification phantoms with three different copper wires (0.2, 0.1 and 0.05 mm in diameter) embedded into a 4% agar gel block. Fig. 2 shows a B-mode image of the calcification phantom with wires 0.05 mm in diameter. Four wires of the same diameter were embedded into each phantom at 1 cm depth and 1 cm intervals, and three phantoms are prepared for each kind of phantom. A polyethylene sheet 0.1 mm thick was positioned just behind the wires. The agar gel contained 1% Tech Polymer particles, spherical polymer particles 7 μm in diameter (Sekisui Plastics Co., LTD.). We simulated in vivo conditions by placing a cutaneous tissue layer taken from a swine 1 cm thick onto the gel block. As a result, wires were positioned at 2 cm depth. The size of a ROI was 1 x 3.5 cm, and each ROI was marked with two stainless needles 0.4 mm in diameter located at the both side of the ROI. The center of a ROI is located at 1.75 cm depth, i.e. the median of the correlation window used for the calculation of the correlation at the center of a ROI is located at 2 cm depth.

In this study five B-mode images were obtained for each phantom. Therefore the performance of the proposed method for each kind of wire was investigated using a total of sixty wires in fifteen B-mode images.

III. RESULTS

Fig. 3 shows the cross-correlation profiles of three ROIs with the wires 0.2, 0.1, and 0.05 mm in diameter, where the intensity threshold parameter α and the stability parameter β are -3 and -10 dB, respectively. The low correlation regions appear at the wire positions and extend along the range direction. The range ambiguity of the proposed indicator is caused by the width of the correlation window. These results imply that the correlation profile is a useful indicator of calcifications with higher sensitivity than acoustic shadowing.

For the investigation of the efficiency of the proposed indicator we examined the sensitivity and the positive predictive value of a calcification detection method using the indicator. Each datum is presented as the average ± the standard deviation, where the sample size is 15. The correlations between scan lines behind a calcification are suppressed continuously along the range direction. Thus the calcification detection method predicts the existence of a calcification when the low correlation region continues more than 0.5 times of the correlation window width along the range direction. Fig. 4 shows the distributions of the sensitivities and the positive predictive values of the calcification detection methods using nine combinations of parameters α and β, where
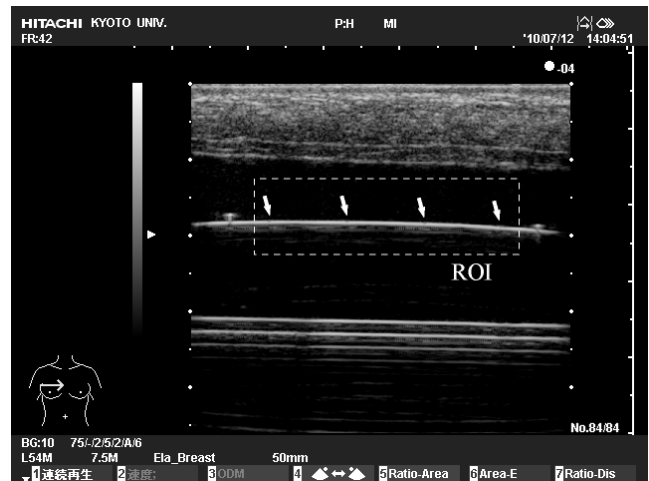

Fig. 2 B-mode image of a calcification phantom with four wires 0.05 mm in diameter. White arrows point at wires, and a white broken line is the boundary of the ROI. Two needles 0.4 mm in diameter were set at both sides of the ROI.
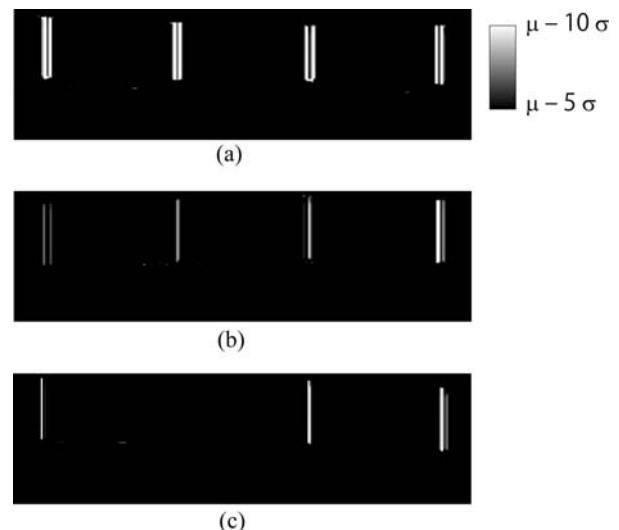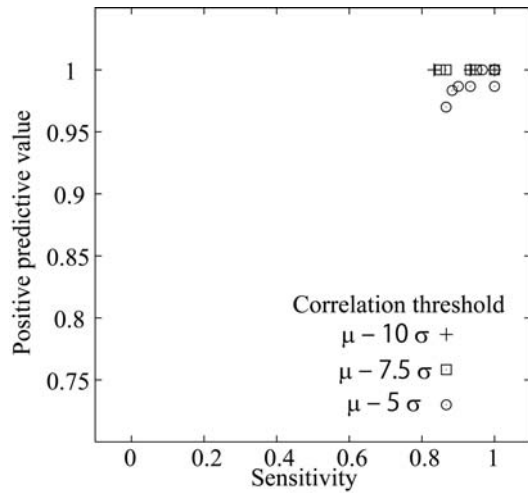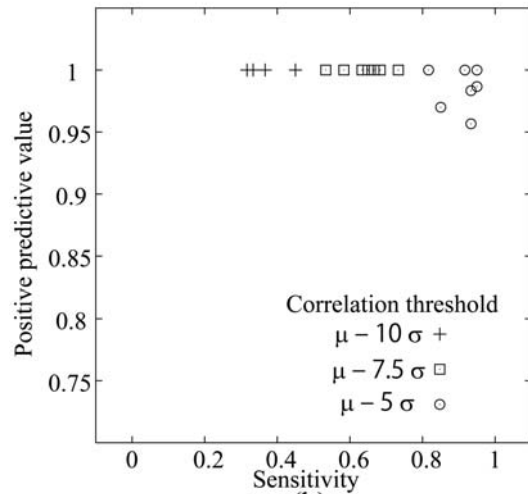

Fig. 3 Normalized cross-correlation profiles of three ROIs with four wires (a) 0.2, (b) 0.1, and (c) 0.05 mm in diameter. The size of each ROI is 1 x 3.5 cm. μ and σ are the average and the standard deviation of the top 90% of the correlation coefficients in each ROI.
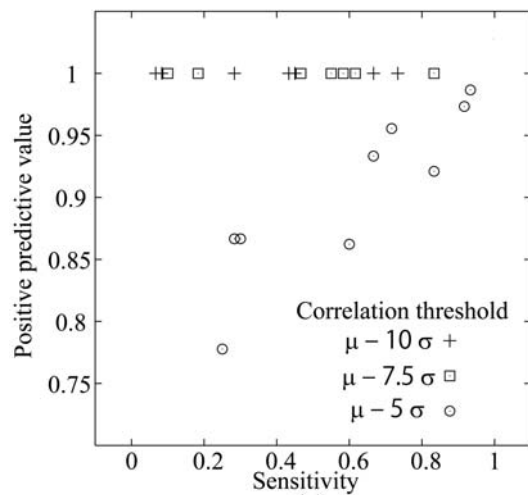
the correlation threshold parameter γ are 10, 7.5, and 5. The severe correlation threshold eliminates false images at the cost of the sensitivity of the method. When the correlation threshold parameter γ of 7.5 was employed, no false image appeared in the nine cases using different combinations of parameters α and β. In addition, the sensitivity of the method for a thin wire largely depends on the parameters α and β. For the solution of the two subjects, the optimization of the parameters α and β and the improvement of the sensitivity of the proposed method, we propose a calcification detection method with a totalizing process. First, the method varies the combination of parameters α and β, where α = 0, -3, and -6 dB and β = 0, -10, and -20 dB. Then the method totals up all the low correlation regions appear in the nine cases of the combinations of parameters α and β.

World Academy of Science, Engineering and Technology
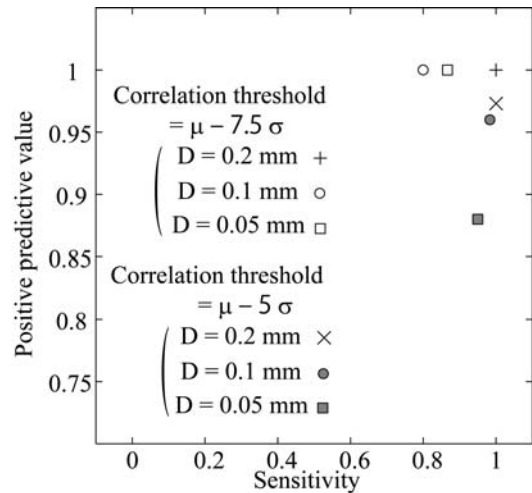International Journal of Biomedical and Biological Engineering
Vol:4, No:11, 2010

Fig. 5 The sensitivity and the positive predictive value of the calcification detection method with a totalizing process.

The method predicts the existence of calcifications using the totalized low correlation regions. Fig. 5 shows the sensitivities and the positive predictive values of the calcification detection method with the totalizing process. When the correlation threshold parameter γ of 7.5 was employed, the proposed calcification detection method with the totalizing process has excellent performance in detecting wires 0.05 mm in diameter with a sensitivity of $86.7 \pm 15.5\%$ and a positive predictive value of $100 \pm 0\%$. When γ of 5 was employed the sensitivity of the proposed method was improved to $95.0 \pm 10.0\%$ at the cost of the decrease of a positive predictive value to $88.0 \pm 13.6\%$. These results suggest the high potential of a calcification detection method employing the proposed indicator in small calcification detection.

IV. CONCLUSION

In this study we propose a novel indicator of a calcification using US without decrease in frame rate. A calcification detection method employing the proposed indicator detected wires 0.05 mm in diameter with a sensitivity of 86.7% and a positive predictive value of 100%. This study implies that the proposed indicator has the potential to approximate the performance of US in calcification detection to that of an X-ray imager, resulting that an US device will become a convenient, safe, and principal clinical tool for the screening of breast cancer.

Fig. 4 Distributions of the sensitivities and the positive predictive values of the calcification detection methods using nine combinations of an intensity threshold parameter and a stability constant parameter. The diameters of wires are (a) 0.2, (b) 0.1, and (c) 0.05 mm. Three correlation thresholds μ – 10σ, μ – 7.5σ, and μ – 5σ are examined.

World Academy of Science, Engineering and Technology
International Journal of Biomedical and Biological Engineering
Vol:4, No:11, 2010

REFERENCES

[1] H. Özdemir, M. K. Demir, O. Temizöz, H. Genchellac, and E. Unlu, "Phase inversion harmonic imaging improves assessment of renal calculi: a comparison with fundamental gray-scale sonography," *J. Clin. Ultrasound.*, vol. 36, pp. 16-19, 2008.

[2] K. A. B. Fowler, J. A. Locken, J. H. Duchesne, and M. R. Williamson, "US for detecting renal calculi with nonenhanced CT as a reference standard," *Radiology.* vol. 222, pp. 109-113, 2002.

[3] P. M. Lamb, N. M. Perry, S. J. Vinnicombe, and C. A. Wells, "Correlation between ultrasound characteristics, mammographic findings and histological grade in patients with invasive ductal carcinoma of the breast," *Clin. Radiol.* vol. 55, pp. 40-44, 2000.

[4] D. Jacob *et al.*, "Analysis of the results of 137 subclinical breast lesions excisions. Value of ultrasonography in the early diagnosis of breast cancer," *J. Gynecol. Obstet. Biol. Reprod.*, vol. 26, pp. 27-31, 1997.

[5] V. P. Jackson, H. E. Reynolds, and D. R. Hawes, "Sonography of the breast. Semin. Ultrasound CT MR," vol. 17, pp. 460-475, 1996.

[6] E. Tohno, D. O. Cosgrove, and J. P. Sloane, *Ultrasound diagnosis of breast diseases*, Elsevier Health Sciences, Edinburg, 1994.

[7] H. Taki, T. Sakamoto, M. Yamakawa, T. Shiina, and T. Sato, "Calculus Detection for Medical Acoustic Imaging using Cross-correlation: Simulation Study," *J Med. Ultrasonics*, vol. 37, pp. 129-135, 2010.

[8] H. Taki, T. Sakamoto, M. Yamakawa, T. Shiina, and T. Sato, "Small calculus detection for medical acoustic imaging using cross-correlation between echo signals," *Proc. IEEE Int. Ultrason. Symp.*, pp. 2398-2401, 2009.

[9] H. Taki, K. Taki, T. Sakamoto, M. Yamakawa, T. Shiina, and T. Sato, "High range resolution medical acoustic vascular imaging with frequency domain interferometry," *Proc. IEEE EMBS*, accepted.